

Mitral Valve Contour Extraction Using Active Contour Models

Paulo J. S. Gonçalves* , J.R. Caldas Pinto**, Mário Ramalho***, J. Queiroz e Melo ****
Escola Superior de Tecnologia de Castelo Branco, Av. do Empresário 6000 Castelo Branco
tel: (072) 3300300 Email: paulosg@mail.telepac.pt

** *Instituto de Eng. Mecânica- Instituto Superior Técnico, Av. Rovisco Pais 1096 Lisboa Codex*
tel: (01) 8417313 Email: mpinto@gcar.ist.utl.pt

*** *Instituto de Eng. Mecânica- Instituto Superior Técnico, Av. Rovisco Pais 1096 Lisboa Codex*
tel: (01) 8417313 Email: mar@gcar.ist.utl.pt

**** *Hospital de St. Cruz, Av. Prof. Reinaldo dos Santos, Carnaxide,*
2795 Linda a Velha, Portugal, tel: 4171981

Abstract: To perform mitral valve contour extraction a software application is presented to support the surgeon in the implant size decision. The system is based on the application, to mitral valve surgery images, of active contour models. First, current repair surgery to mitral valve disease is discussed. Active contour models are presented and using different implementation approaches a comparison was done. The algorithms proposed by Kass, Amini, Cohen, Eviatar and Shah (Greedy algorithm) were implemented in test environment. The implementation to be used in the software application, is the one due to Kass with a few modifications related to Cohen's approach. During surgery, the system needs to be calibrated and the active contour initialised. These processes are supported by a colour segmentation technique, tested with real images, using fuzzy sets. Real open-heart surgery images have been used to test the system developed.

Keywords: Mitral Valve; Active Contour; Camera Calibration; Colour Segmentation; Fuzzy Sets.

1. Introduction

Computer vision techniques to on-line support surgery has becoming increasingly used. The main reasons are related to the improved cameras and frame-grabbers performance and the increased power of low cost computers. In this work is presented a software application to perform in surgery evaluation of the mitral valve contour and its parameters. The system is based on images taken by a video camera attached to the surgery illumination system, and to be used as an aid to the surgeon. This requires that the image acquisition (true colour), system calibration, colour segmentation and mitral valve measures be performed on-line during open-heart surgery. The ultimate goal is to obtain an implant size decision support tool to be used by the surgeon.

Image processing tools improve surgery techniques. Mitral valve parameters are needed to define the implant

size of the diseased valve that will be replaced to avoid regurgitation [7]. Some works have been made [7] with classic methods not yielding the desired results, what encouraged us to try a different approach.

Active Contour Models have been used with magnetic resonance images [5], [6], [8], [9] and echocardiography images [4]. We apply active contour models to mitral valve surgery images.

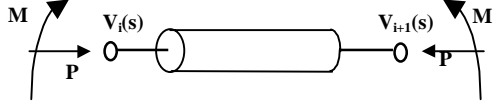
The remainder of this paper will present active contour model theory from the original to some more recent approaches. Different algorithms were implemented to test its behaviour and determine what will be used in the system to extract mitral valve contour. Criteria were defined to compare the different algorithms. The set of criteria is related to computational effort, the parameters setting simplicity, the active contour model initialisation and results in test images.

To help finding the calibration target is used colour segmentation. A novel approach is presented supported with fuzzy sets to find green tones for the example exposed. To test the method true colour, micro-heart surgery images taken with micro remote head colour CCD cameras were used.

2. Active Contour Model

2.1. The Energy Model

An Active Contour [15] is a model of a deformable curve. In the discrete case, a set of image points named control points. Those points are self connected by an elastic virtual component rod. These components enables traction/compression and flexion behaviour. A physical model is presented.



Active Contour Model is defined as a deformable contour mapping over the 2-dimensional space:

$$\Omega = [0,1] \rightarrow \mathfrak{R}^2$$

$$s \rightarrow v(s) = (x(s), y(s))$$

The model has a space of admissible deformations Ad , when the functional $J(v(s))$ is minimised. The functional depends on the internal, image and constraint energies.

$$J: Ad \in \mathfrak{R}^2 \rightarrow \mathfrak{R}$$

$$v(s) \rightarrow J(v(s)) = E_{\text{internal}}(s) + E_{\text{image}}(s) + E_{\text{constraint}}(s)$$

The space of admissible deformations is restricted to the Active Contour boundary constraints, which vary depending on the contour shape, open or closed.

To the referred energies is attached a potential and a force, since:

$$E(v(s)) = \int_{\Omega} P(v(s)) ds \quad \text{e} \quad F(v) = -\nabla P(v)$$

If $v(s)$ is a local minimum of $J(v(s))$, the Lagrange equation is satisfied and a force equilibrium is accomplished over the Active Contour, static case.

$$F_{\text{internal}}(s) + F_{\text{image}}(s) + F_{\text{constraint}}(s) = 0$$

From a initial position, the Active Contour tries to reach a local minimum, ruled by the dynamic equation:

$$\gamma \cdot \frac{\partial^2 v(s)}{\partial t^2} + \mu \cdot \frac{\partial v(s)}{\partial t} = F_{\text{internal}}(s) + F_{\text{image}}(s) + F_{\text{constraint}}(s)$$

When $v(s)$ reaches a local minimum, equilibrium is obtained and the static equation is verified.

2.2. Forces Applied to the Model

2.2.1. Internal forces

Elastic forces promote the active contour traction/compression. The physical model analogy denotes that consecutive control points connected by a linear spring evolve to a single point. This force denotes distance minimisation of two consecutive control points.

$$F_{\text{elastic}}(s) = K(\Delta x - L_0)^2 \quad \text{and} \quad E_{\text{elastic}} = \frac{1}{2} \cdot \int_0^1 \alpha(s) \cdot \left| \frac{\partial v(s)}{\partial s} \right|^2 ds$$

Flexion forces promote contour smoothing. When a momentum is applied to the rod extremes, a curvature is verified and the contour is smoothed.

$$E_{\text{flexion}} = \frac{1}{2} \cdot \int_0^1 \beta(s) \cdot \left| \frac{\partial^2 v(s)}{\partial s^2} \right|^2 ds$$

2.2.2. Image Forces

To attract the active contour to image features some forces need to be defined, depending on what we are extracting from the image.

The gradient force enables active contour attraction to high gradient regions, and its potential is defined:

$$P(v(s)) = -|\nabla I(v(s))|^2$$

The grey-level force enables the active contour attraction to pre-defined grey-levels:

$$P(v(s)) = I(v(s))$$

The edge force enables the active contour attraction to pre-defined edges:

$$P(v(s)) = |I_{\text{edges}}(v(s))|$$

Cohen [5] defined the balloon force, which enables the active contour to expand. This force enables contour initialisation inside the contour to extract.

$$F_n(s) = K_1 \cdot n(s)$$

2.2.3. Constraint Forces

These forces introduced by Kass [15] disable active contour free movement. This characteristic is used to prevent unwanted local minima and to help finding the optimal solution. Vulcan force repulses the contour from unwanted image pixels and spring constraint attracts the contour to desired image pixels.

2.3. The Discrete Model

Active contour dynamic equation discretisation is done in time and space domains. The spatial step $h(s)$, is the distance between consecutive control points. Time discretisation is done by discrete values t , separated with time step τ .

Finite difference method was used to obtain the discretisation. Progressive and central finite differences, to 1st and 2nd order spatial derivatives and regressive for

time discretisation. Finite element method was not used because the problem is not 3D and very difficult [6].

The discrete equation is obtained considering $\gamma=0$, a system of n -number of control points equations.

$$(I + \tau \cdot K) \cdot v^t = v^{t-1} + \tau \cdot F(v^{t-1})$$

where,

- K, represents the active contour rigidity matrix;
- F, represents image and constraint forces;
- I, represents the identity matrix;
- v, represents the active contour.

$$K = \frac{1}{h^4} \begin{bmatrix} A_1 & B_2 & C_3 & & & & C_{N-1} & B_N \\ B_1 & A_2 & B_3 & C_4 & & & & C_N \\ C_1 & B_2 & A_3 & B_4 & C_5 & & & \\ & C_2 & B_3 & A_4 & B_5 & C_6 & & \\ & & & \ddots & & & & \\ & & & & C_{N-4} & B_{N-3} & A_{N-2} & B_{N-1} & C_N \\ C_{N+1} & & & & C_{N-3} & B_{N-2} & A_{N-1} & B_N \\ B_{N+1} & C_{N+2} & & & C_{N-2} & B_{N-1} & A_N \end{bmatrix}$$

where:

$$\begin{aligned} A_s &= 2 \cdot \alpha \cdot h^2 + 6 \cdot \beta \\ B_s &= -(\alpha \cdot h^2 + 4 \cdot \beta) \\ C_s &= \beta \\ s &\in \{1, 2, \dots, N-1, N\}, \text{ control point index.} \end{aligned}$$

2.4. Boundary Conditions

There are two kinds of boundary conditions, one denoted to the active contour nature and other to the image. If the active contour is closed, continuity between extreme and internal control points must be verified. If it is open only internal continuity must be verified. The active contour movement is also constrained by the image boundaries.

2.5. Active Contour Initialisation

There are mainly two types of active contour initialisation, the manual and the automatic. The manual produces better results because the operator controls all the inputs, but an automatic one is preferable however produces worse results.

Manually we can initialise the active contour outside or inside the contour to extract, depending on the algorithm used. Lai [14] proposed the Hough transform to automatically initialise the active contour.

2.6. Implementation Algorithms

Since the original active contour algorithm that various implementations have been developed. In this work we only present the most generic ones. Several authors

produced other algorithms more dedicated to their problems, [6], [2], [13], [8], [4], [12], [3].

2.6.1. Kass Modified Algorithm

This algorithm was presented in the past sections, but some modifications must be done related to Cohen's approach. Such modifications are important due to numerical instability produced by time discretisation. The term $\tau \cdot F(v^{t-1})$ can cause the active contour to over-pass the solution due to large values of τ . Cohen [5] proposed normalising the image forces.

$$F_{image} = -\frac{\nabla P}{\|\nabla P\|}$$

In objects, where the boundary is of "strong" transition, the active contour can over-pass the solution. To solve the problem, Cohen [5] smoothed the object boundary using a Gaussian filter.

$$F_{image} = G(n) \otimes F_{image}$$

2.6.2. Amini Algorithm

Amini [1] proposed to minimise active contour global energy by minimising local energy at each control point.

$$E(v_1, v_2, \dots, v_i, \dots, v_N) = E(v_1, v_2) + E(v_2, v_3) + \dots + E(v_i, v_{i+1}) + \dots + E(v_{N-1}, v_N)$$

Dynamic programming calculates a sequence of functions s_i at each control point to obtain local minimisation. The following recurrent formula is obtained for active contour.

$$\begin{aligned} s_i(v_{i+1}, v_i) &= \min_{v_{i-1}} (s_{i-1}(v_i, v_{i-1}) + \alpha \cdot (|v_i - v_{i-1}|)^2 + \\ &+ \beta \cdot (|v_{i+1} - 2 \cdot v_i + v_{i-1}|)^2 + E_{\text{externa}}(v_i)) \end{aligned}$$

2.6.3. Cohen Algorithm

Cohen [5] proposed a new image force, which makes the active contour evolution less dependent from initialisation because it now expands. The balloon force causes the expansion.

The normal vector at each control point $n(v(s))$, is multiplied by a constant parameter controlling the intensity.

2.6.4. Eviatar Algorithm

Eviatar algorithm proposed by Eviatar [9], does not use derivatives to express the internal active contour energy because it is discrete identity.

$$E_{internal}(i) = k(i) \left[|v_i - v_{i+1}| - r_i \right]^2$$

where:

- i, control point index;
- $k(i)$, controls active contour elasticity;
- $v(i)$, represents the i^{th} control point;
- $r(i) = |v_i - v_{i+1}|$, equilibrium term between control points.

Active contour global energy is calculated as a sum of all control points local energy.

$$E = \sum_{i=0}^{N-1} \left[E_{internal}(i) + E_{image}(i) \right]$$

2.6.5. Greedy Algorithm

The author [16] proposed new formulation for some energetic terms of the base theory. Minimising the elastic energy the control points became evenly spaced.

$$E_{elastic} = (d_{med} - |v_i - v_{i-1}|)^2$$

d_{med} – mean distance between control points.

Image energy based on the gradient, is computed as follows for each control point:

$$E_{image} = \frac{\min - \text{mag}}{\max - \min}$$

min, max – values for control points in the neighbourhood.

mag – magnitude of the gradient.

This method can include information about active contour corners. When a corner is found there is no need to smooth the curve, so the corners can be formed. When c_i become superior to a threshold value a corner is detected and the flexion force must be zeroed to form that corner.

$$c_i = \left| \frac{\vec{u}_i}{|\vec{u}_i|} - \frac{\vec{u}_{i+1}}{|\vec{u}_{i+1}|} \right|^2$$

3. Algorithms Comparison

Tests were made under *Matlab*TM4.2.c with a Intel's 166Mhz processor and 32Mb RAM. Tests were made with a real image and a final conclusion should be accomplished regarding a future implementation for mitral valve contour extraction.

3.1. Comparison Criteria

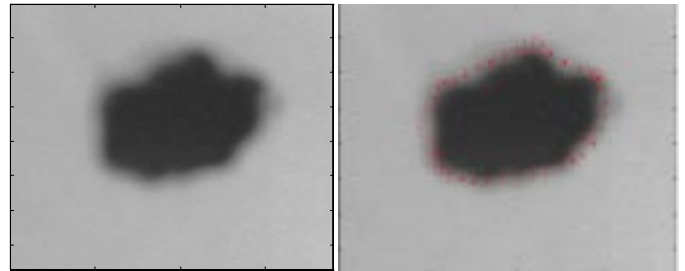
The following criteria must be evaluated for each algorithm to build a summary comparison table and withdraw some conclusions.

Computational effort is nowadays an important design factor for any automatic system. *Flops* per number of control points by iteration will measure the computational effort of the algorithm. This criterion is important since much information needed for an algorithm to get an optimal solution can slow the process.

Many parameters setting can difficult the algorithm finding the optimal solution but give it more degrees of freedom. There is always a compromise solution to be made between image and internal forces.

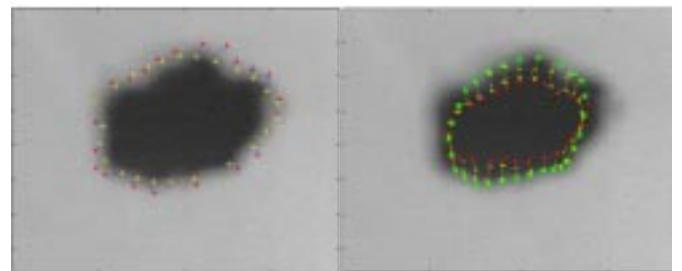
Active contour initialisation done with correct criteria can cause good results. As much closer from the optimal solution better results we get. There are internal, inside the object to detect, or external initialisation depending on the algorithm to be used.

Another criteria are the results presented for the next test image for the five algorithms tested. We have pursuit the contour initialisation that enables the results expected. Further tests in [11].



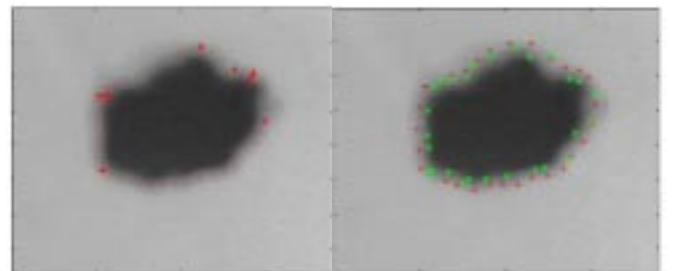
Test image

Kass solution



Amini solution

Cohen solution



Greedy solution

Eviatar solution

	Computational Effort [flops / control points]	Parameters	Initialisation [Int. vs Ext.]	Results
Kass	3703	$\tau, \alpha, \beta, \gamma$	External	- corners + precision
Amini	12655	α, β, γ, n	External	- precision - corners
Cohen	3927	$\tau, \alpha, \beta, \gamma, k$	Internal	- corners - precision
Greedy	519	$\alpha, \beta, \gamma, c, t, n$	External	- precision + corners
Eviatar	464	α, γ, n	External	- precision - corners

This summary table and tests are more detailed in [11], where other images were tested.

The chosen algorithm for mitral valve contour extraction is the Kass-modified. It yields good precision and it is satisfactorily fast, the best compromise between the algorithms to accomplish mitral valve contour extraction.

4. Mitral Valve Contour Extraction

Mitral Valve Contour Extraction is accomplished by processing a colour image captured during open-heart surgery. The camera used is attached to the surgery room illumination system and a Matrox® Meteor capture board is placed on an Intel's Pentium 166MHz. The software application developed then processes the captured image. This process is considered done when three steps were accomplished; finding a good image, camera calibration and active contour model application. For camera calibration green colour segmentation is needed to define the calibration target points. Active contour model application is done in a system developed to work in on-line open-heart surgery.

4.1. Colour Segmentation

Due to the difficulty on finding the right green tone to perform segmentation we introduce the fuzzy set concept to colour segmentation. Among all possible RGB values "Pure green" is defined as [0 255 0].

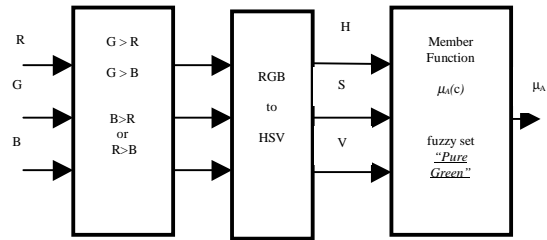
In order to build the fuzzy set for green tones we need to define a member function to that set. Each possible tone of green as a different membership grade, between 0 and 1, which denotes the proximity to "Pure green". The current technique can also be applied to red, yellow, cyan, blue, magenta, white and black colours.

Defining a colour c , from the RGB space with all 256^3 possible colours the fuzzy set "Pure green" A , is defined as follows:

$$A = \left\{ (c, \mu_A(c)) \mid c \in RGB \right\}$$

At each colour c , corresponds a membership grade defined by the member function $\mu_A(c)$. "Pure green" has $\mu_A=1$ and the other green tones $1 > \mu_A(c) \geq 0$.

The next figure represents how image colours are processed to find the correspondent membership grade to the green tone fuzzy set. The first block filters image colours to obtain only green tones.



The second block green tones are transformed from the RGB model to the HSV model [10] to obtain information about the colour tones. *Hue* represents the different colours, *Saturation* defines how far is the equal intensity grey level and *Value* represents colour intensity from the colour distinguished by *Hue*. This model expose information about image colours simplifying member function $\mu_A(c)$ finding.

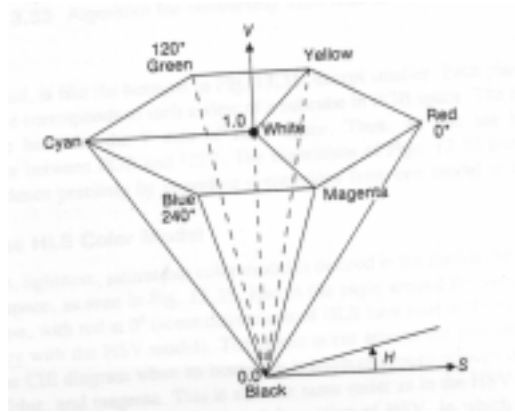
We propose a member function to obtain the *green tone* fuzzy set. The membership grade is determined by multiplying the normalised H, S and V components. For green tones $H \in [1/6; 3/6]$ so normalisation is needed and determined as shown in the equation.

$$\mu_A(c) = \begin{cases} \left[\frac{H}{1/6} - 1 \right] \times S \times V & , \text{ if } 1/6 < H < 2/6 \\ \left[3 - \frac{H}{1/6} \right] \times S \times V & , \text{ if } 2/6 \leq H < 3/6 \\ 0 & , \text{ if } 3/6 \leq H \leq 1/6 \end{cases}$$

where,

$$\begin{aligned} H &\in [0;1] \\ S &\in [0;1] \\ V &\in [0;1] \end{aligned}$$

Symmetry is found around $H=2/6$ in the member function. To distinguish between blue toned greens and yellow toned greens we must specify in the first block of the processing method what kind of "green tone" do we want to obtain.



HSV model [10]

Given a membership grade-green tone interval, we can obtain green colour image segmentation as we can verify in next section.

4.2. Colour Segmentation Results

We tested the proposed method in 16 million colour real heart images in the application developed to extract mitral valve contour.

Given the test image a), total green colour segmentation was accomplished in image b). Different membership grades were tested in order to extract only calibration targets green tones, image c). Image d) represents tones closest to “pure green” obtained by reducing membership grade interval.

We can conclude that the majority of green tones correspond to membership grades near to zero, since “pure green” is very difficult to obtain in real images.



Image a)

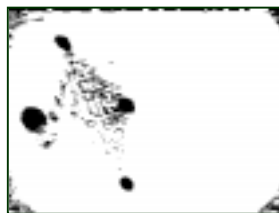


Image b)

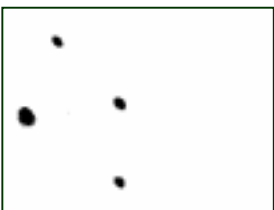


Image c)

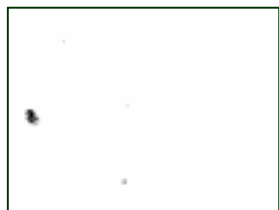


Image d)

b) $0 < \mu_A \leq 1$; c) $0.1 < \mu_A \leq 1$; d) $0.3 < \mu_A \leq 1$.

4.3. Active contour application

The system developed for mitral valve contour extraction using active contour models offers satisfactory results, presented in this section for open-heart images. Images are captured and processed on-line during surgery, giving the surgeon a new tool for implant size calculations.

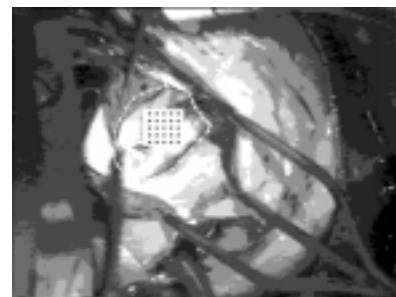


MitralApp – active contour application

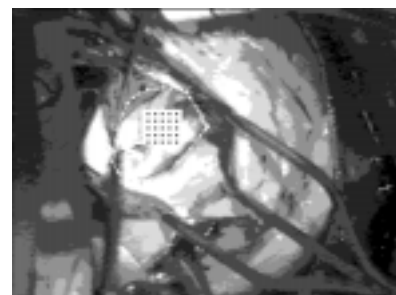
Active Contour was manually initialised near the optimal solution, using the system developed. Contour parameters were settled to perform a better attachment to the mitral valve contour,

$$\alpha(s) = h^2 \text{ and } \beta(s) = h^4$$

due to coefficient matrix K [5]. In some images these parameters need to be modified in order to stand-up the image force weight and obtain a better attachment to image features. Since the mitral valve contour is very irregular the image forces must overcome the internal forces to form sharp edges. Two result images are presented and we can verify that making $\beta(s)$ three times greater the task is accomplished.



$\beta(s)$



$3 \times \beta(s)$

5. Conclusions And Future Work

In this paper we presented a software application to perform evaluation of the mitral valve contour and its parameters during surgery.

The system developed can capture and process a mitral valve surgery image. Before processing, the system must be calibrated and the active contour initialised. These techniques were supported by colour segmentation due to image complexity.

A first approach to colour segmentation was done to segment green tones from the calibration target. A fuzzy set based theory was presented who held satisfactory results, but need to be further refined.

As a result from active contour model implementation the Kass-modified algorithm was used to extract mitral valve contour in the system developed. It yields good results but active contour initialisation is manual. A refined colour segmentation technique and colour initialisation will allow to fully automating implant size decision tool.

6. References

- [1] A. Amini, T. Weymouth, R. Jain, "Using Dynamic Programming for Solving Variational Problems in Vision", in *IEEE Trans. Pattern Anal. Machine Intell.*, vol. 12, n°9, pp. 855-867, Sep. 1990
- [2] A. M. Baumberg, D. C. Hogg, "An Efficient Method for Contour Tracking using Active Shape Models", Research Report Series 94.11, School of Computer Studies, University of Leeds, April 1994
- [3] V. Caselles, R. Kimmel, G. Sapiro, "Geodesic Active Contours", *Int. Journal of Computer Vision*, 22(1), pp.61-79, 1997
- [4] V. Chalana, D.T. Linker, D.R. Haynor, Y. Kim, "A Multiple Active Contour Model for Cardiac Boundary Detection on Echocardiographic Sequences", in *IEEE Trans. Medical Imaging*, vol. 15, n°3, pp. 290-298, June 1996
- [5] L. Cohen, "Note on Active Contour Models and Ballons", *CVGIP: Image Understanding*, vol. 53, n°2, pp. 211-218, 1991
- [6] L. Cohen, I. Cohen, "Finite-Element Methods for Active Contours Models and Ballons for 2-D and 3-D images", in *IEEE Trans. Pattern Anal. Machine Intell.*, vol. 15, n°11, pp. 1131-1147, Nov. 1993
- [7] M. Costa, E. M. Luís, J.R. Caldas Pinto, J. Queiroz e Melo, "Mitral Valve Measurements During Cardiac Surgery", *BioEng'94 III Portuguese Congress on Biomedical Engineering*, Porto 24-26 November 1994, Portugal
- [8] C. A. Davatzikos, J. L. Prince, "An Active Contour Model for Mapping the Cortex", in *IEEE Trans. Medical Imaging*, vol. 14, n°1, pp. 65-80, March 1995
- [9] H. Eviatar, R. L. Somorjai, "A Fast, Simple Contour Algorithm for Biomedical Images", in *Pattern Recognition Letters*, 17, pp. 969-974, 1996
- [10] J.D. Foley, A. van Dam, S.K. Feiner, J.F. Hughes, "Computer Graphics - principles and practice", Addison-Wesley, 1990
- [11] P.S. Gonçalves, "Extracção e Medição dos Contornos da Válvula Mitral utilizando Modelos Activos de Contornos", Msc thesis submitted at Instituto Superior Técnico, Lisbon, Portugal, January 1998
- [12] S.R. Gunn, M.S. Nixon, "A Robust Snake Implementation: A Dual Active Contour", in *IEEE Trans. Pattern Anal. Machine Intell.*, vol. 19, n°1, pp.63-68, Jan 1997
- [13] K.F. Lai, R.T. Chin, "On regularization, formulation, and initialisation of active contour models(snakes)", *Asian Conf. Computer Vision*, pp.542-545, 1993
- [14] K. F. Lai, R.T. Chin, "Deformable Contours: Modelling and Extraction", in *IEEE Trans. Pattern Anal. Machine Intell.*, vol. 17, n°11, pp.1084-1090, Nov. 1995
- [15] M. Kass, A. Witkin, D. Terzopoulos, "Snakes: Active Contour Models", *First Int. Conf. on Comp. Vision*, London, pp. 259-268, June 1987
- [16] D. Williams, M. Shah, "A Fast Algorithm for Active Contours and Curvature Estimation", in *CVGIP: Image Understanding*, vol. 55, n°1, pp. 14-26, 1992